Decomposition of higher-order homogeneous tensors and applications to HARDI

Document status and date:
Published: 01/01/2012

Document Version:
Publisher's PDF, also known as Version of Record (includes final page, issue and volume numbers)

Please check the document version of this publication:

• A submitted manuscript is the version of the article upon submission and before peer-review. There can be important differences between the submitted version and the official published version of record. People interested in the research are advised to contact the author for the final version of the publication, or visit the DOI to the publisher's website.
• The final author version and the galley proof are versions of the publication after peer review.
• The final published version features the final layout of the paper including the volume, issue and page numbers.

[Link to publication](#)

CDMRI 2012

MICCAI 2012 workshop on Computational Diffusion MRI

Held in Conjunction with MICCAI 2012
Nice, France, October 5th, 2012.

http://cmic.cs.ucl.ac.uk/cdmri12/

Organizers:

Eleftheria Panagiotaki	University College London, UK
Lauren O'Donnell	Harvard Medical School, USA
Thomas Schultz	MPI Intelligent Systems, Germany
Gary Hui Zhang	University College London, UK

Decomposition of Higher-Order Homogeneous Tensors and Applications to HARDI

E. Balmashnova, A. Fuster and L.M.J. Florack

Eindhoven University of Technology, The Netherlands
E.Balmachnova@tue.nl

Abstract. High Angular Resolution Diffusion Imaging (HARDI) holds the promise to provide insight in connectivity of the human brain in vivo. Based on this technique a number of different approaches has been proposed to estimate the fiber orientation distribution, which is crucial for fiber tracking. A spherical harmonic representation is convenient for regularization and the construction of orientation distribution functions (ODFs), whereas maxima detection and fiber tracking techniques are most naturally formulated using a tensor representation. We give an analytical formulation to bridge the gap between the two representations, which admits regularization and ODF construction directly in the tensor basis.

1 Introduction

Diffusion MRI provides information about the fiber structure of brain white matter in a noninvasive way. It is based on the measurement of the Brownian motion of water molecules in tissue, which can be related to the tissue's microstructure. In the last decade several techniques have been proposed, from Diffusion Tensor Imaging (DTI) [1,2] to the more general High Angular Resolution Diffusion Imaging (HARDI) [3]. In order to perform classification or fiber tracking one needs accurate estimation of the orientation distribution function (ODF) from the original HARDI signal.

Most HARDI approaches are based on two alternative function representations on the sphere. The first one is the well-known spherical harmonic decomposition [4,5] and the second one is the homogeneous tensor decomposition proposed by Özarslan and Mareci [6]. These representations have the same number of basis functions and span the same vector space provided that the rank of the tensor representation equals the spherical harmonics highest order. Each has its pros and cons. The spherical harmonic representation permits efficient ways of computing the ODF from the data, as demonstrated in the context of the diffusion orientation transform (DOT) [7], and Q-ball technique and its generalizations [8,9,10]. It also permits regularization in a relatively straightforward way [11,12,13]. On the other hand, the tensor representation attracts nowadays more and more attention due to applications such as ODF maxima extraction [14,15], the computation of rotationally invariant scalar measures [16,17,18] and for parametrization of the space of positive-definite higher-order tensors [19,20]. The tensorial representation offers the additional advantage that it has the natural format for a Finsler geometric

approach towards HARDI tractography and connectivity analysis [21,22,23]. On the other hand, the initial step of obtaining the diffusion ODF requires a SH representation, after which a linear transformation to a tensor description is performed [24]. Florack and Balmashnova [12] offer a third representation, based on an inhomogeneous tensor decomposition. Their representation reconciles the tensor representation with the regularization rationale obviating the need for an intermediate spherical harmonic decomposition. A first attempt to construct the diffusion ODF directly in tensor basis was recently presented [25]. Their recipe requires lengthy manual derivation for each tensor order, which becomes very cumbersome for high orders. In this work, however, we present an analytic approach.

In this paper we describe how to obtain the diffusion ODF (Q-ball and constant solid angle) and regularization analytically for a tensor representation of arbitrary order directly from data evidence, by fitting a homogeneous tensor to the data and then analytically decomposing the resulting homogeneous tensor in order to benefit from the inhomogeneous representation. The final algorithm for regularization or ODF computation is based on simple matrix multiplication of the tensor coefficients.

2 Higher-Order Tensor Representations

An interesting alternative to spherical harmonics is provided by a higher-order tensor representation (higher than order two). Originally Özarslan and Mareci [6] proposed a homogeneous high-rank tensor representation[1]

$$S_n^{\mathrm{hom}}(y) = D^{i_1 \dots i_n} y_{i_1} \dots y_{i_n}, \tag{1}$$

where $y = (y_1, y_2, y_3)$ is a unit vector and D is a higher-order diffusion tensor of rank n. This is a generalization of the diffusion tensor model in which a 2-rank tensor is used. These high-rank Cartesian diffusion tensors can be computed avoiding the computationally costly spherical harmonics. Regularization plays a very important role for robustness purposes. In case of a homogeneous high-rank tensor representation, the only explicit type of regularization that is easily enforced is by constraining the rank (lower rank implies higher degree of regularization) as explained in [26]. In fact, DTI is reasonably robust because of the 2nd order rank constraint explicitly built in. The alternative inhomogeneous higher-order tensor decomposition resolves this robustness problem by exploiting redundancy of the polynomial basis on the sphere in such a way that terms of the same order in the resulting decomposition become eigenfunctions under regularization [12]. The nonregularized data decomposition has the form

$$S_n^{\mathrm{inhom}}(y) = \sum_{j=0}^{n} D^{i_1 \dots i_j} y_{i_1} \dots y_{i_j} \tag{2}$$

in the redundant basis of polynomials $\{y_{i_1} \dots y_{i_j} \mid j = 0, 2, \dots n\}$ on the unit sphere[2]. The idea is to encode in the higher-order part the residual information which cannot

---

[1] Here and henceforth summation convention for repeated indices applies.

[2] It is assumed that $S_n(y) = S_n(-y)$, whence only even order monomials are used.

be revealed by lower-order terms. The algorithm for computing the coefficients has a hierarchical structure [12]:

1. D^0 is found by minimization of the energy (Ω denotes the unit sphere, and $\mathrm{d}\Omega$ the appropriate measure)

$$E_0(D^0) = \int_\Omega (S(y) - D^0)^2 \mathrm{d}\Omega, \qquad (3)$$

2. If all terms of order up to $j-1$ are known, the j-th order coefficients are obtained from minimization of the energy

$$E_j(D^{i_1 \cdots i_j}) = \int_\Omega ((S(y) - \sum_{k=0}^{j-1} D^{i_1 \cdots i_k} y_{i_1} \ldots y_{i_k}) - D^{i_1 \cdots i_j} y_{i_1} \ldots y_{i_j})^2 \mathrm{d}\Omega \quad (4)$$

The solution requires only one data term of the resulting linear system to be computed numerically, analytic expressions for all other integrals are given in [12]. Although both tensor decompositions, homogeneous and inhomogeneous, are equivalent on the sphere in the sense that $S_n^{\mathrm{inhom}}(y) = S_n^{\mathrm{hom}}(y)$, the inhomogeneous one has important advantages. It allows to regularize and construct the ODF directly, without going to a spherical harmonics basis. This is possible due to the following properties:

1. The polynomials $D^{i_1 \cdots i_k} y_{i_1} \ldots y_{i_k}$ for fixed k belong to the span $\{Y_{km}(y), m = -k, \ldots, k\}$ of the spherical harmonics of the same order k.
2. The polynomials $D^{i_1 \cdots i_k} y_{i_1} \ldots y_{i_k}$ are eigenfunctions of the Laplace-Beltrami operator $\triangle_{\mathrm{LB}}$, thus in practice they are easily regularized by Tikhonov regularization [11,12].
3. $S_n^{\mathrm{inhom}}(y, t)$ satisfies the heat equation on the unit sphere with the initial condition $S_n^{\mathrm{inhom}}(y, 0) = S_n^{\mathrm{inhom}}(y)$.

However, the inhomogeneous representation also poses a few drawbacks:

1. Due to the fact that the algorithm requires several steps with least squared fittings, it is less robust compared to one for the homogeneous representation.
2. It requires to store more coefficients for each point. Instead of the $(n+1)(n+2)/2$ coefficients required in the homogeneous case, $(n + 2)(n + 4)(2n + 3)/24$ are needed, unless one is able to make all mutual dependencies among the coefficients explicit beforehand (which is not an easy task).

3 Decomposition of Homogeneous Tensors

Starting point is a homogeneous tensor representation, Eq. (1), fitted to HARDI data (see, for example, [27]). We propose to decompose such a homogeneous tensor into the inhomogeneous representation given by Eq. (2). Instead of tensor index notation

we adopt the multi-index notation used in [19]. The signal S can then be written as a homogenous polynomial of even order n:

$$S_n^{\text{hom}}(y) = \sum_{|\alpha|=n} D_\alpha y^\alpha = \sum_{\alpha_1+\alpha_2+\alpha_3=n} D_{\alpha_1\alpha_2\alpha_3} y_1^{\alpha_1} y_2^{\alpha_2} y_3^{\alpha_3} \tag{5}$$

For implementation purposes we store the coefficients in Eq. (5) as a $\frac{1}{2}(n+1)(n+2)$-dimensional vector $\mathbf{D}$ and the monomials as a vector $\mathbf{v}$, so that

$$S_n^{\text{hom}}(y) \overset{\text{def}}{=} \mathbf{D}^T\mathbf{v}. \tag{6}$$

For example, in the case $n = 2$, $\mathbf{v}^T = (y_1^2, y_1y_2, y_2^2, y_2y_3, y_3^2, y_1y_3)$. Given such a homogeneous polynomial matched to the data S we now wish to map the known coefficients D_α to coefficients $D_\alpha^{2\nu}$ of the aforementioned equivalent inhomogeneous representation[3], Eq. (2), in such a way that $D_n^{2\nu}(y)$ belongs to the span of spherical harmonics of order 2ν:

$$S_n(y) = S_n^{\text{inhom}}(y) \overset{\text{def}}{=} \sum_{\nu=0}^{n/2} D_n^{2\nu}(y). \tag{7}$$

The vectors of coefficients are related by

$$\mathbf{D} = \sum_{\nu=0}^{n/2} \mathbf{D}^{2\nu}. \tag{8}$$

Any polynomial can be decomposed into a sum of harmonic polynomials h_l, as follows:

$$S_n(y) = \sum_{\nu=0}^{n/2} r^{n-2\nu} h_{2\nu}(y) \tag{9}$$

where h_l is a homogeneous harmonic polynomial of order l (i.e. $\triangle h_l(y) = 0$, where $\triangle$ is the Laplacian operator in 3D) and $r^2 = y_1^2 + y_2^2 + y_3^2$. The property of spherical harmonics being homogeneous harmonic polynomials on the unit sphere is of crucial importance, since it allows us to transfer well-developed algorithms for HARDI relative to a spherical harmonic basis to the inhomogeneous polynomial basis. This allows us to conclude that the polynomial $r^{n-k}h_k$ restricted to the unit sphere for fixed k belongs to the span of the spherical harmonics of the same order, $\{Y_{km}(y),\ m = -k, \ldots, k\}$. The polynomial $r^{2\nu}h_{n-2\nu}$ is explicitly given by [28]:

$$r^{n-2\nu} h_{2\nu} = \frac{(4\nu+1)!!}{(n-2\nu)!!(n+2\nu+1)!!} \sum_{\mu=0}^{\nu} \frac{(-1)^\mu (4\nu-2\mu-1)!!}{(2\mu)!!(4\nu-1)!!} r^{2(\mu+\frac{n}{2}-\nu)} \triangle^{\mu+\frac{n}{2}-\nu} S_n(y) \tag{10}$$

We derive the exact formula by substituting Eq. (5) into Eq. (10) and using the binomial expansions for both $r^{n-2(\nu-\mu)}$ and $\triangle^{\frac{n}{2}-(\nu-\mu)}$, with changes in the order of summation[4]

$$D_n^{2\nu}(y) \overset{\text{def}}{=} r^{n-2\nu} h_{2\nu} = \sum_{|\alpha|=n} D_\alpha^{2\nu} y^\alpha \tag{11}$$

---

[3] The reverse mapping from inhomogeneous to homogeneous representation is trivial by inserting powers of $r^2 = y_1^2 + y_2^2 + y_3^2$ into the monomials in Eq. (5).

[4] Caveat: α is multi-index, n is integer, so $D_n^{2\nu}(y)$ and $D_\alpha^{2\nu}$ should not be confused.

where for all $|\alpha| = n$ (cf Eq. (5))

$$D_\alpha^{2\nu} = \sum_{|\beta|=n} D_\beta c_\alpha^{2\nu,\beta}, \tag{12}$$

$$c_\alpha^{2\nu,\beta} = \frac{(4\nu+1)!!}{(n-2\nu)!!(n+2\nu+1)!!} \sum_{\mu=0}^{\nu} (-1)^\mu \sum_{|\gamma|=\mu+\frac{n}{2}-\nu}^{*} \frac{(4\nu-2\mu-1)!!((\mu+\frac{n}{2}-\nu)!)^2 \beta!}{(2\mu)!!(4\nu-1)!!\gamma!(\alpha-\beta+2\gamma)/2)!(\beta-2\gamma)!} \tag{13}$$

where $*$ means that summation applies only for the terms for which the following conditions are satisfied:

$$(\beta - \alpha \le 2\gamma \le \beta) \quad \text{and} \quad (\alpha_i - \beta_i \text{ even}), \tag{14}$$

Note that in multi-index notation $\alpha! = \alpha_1!\alpha_2!\alpha_3!$, and $\alpha < \beta$ implies $\alpha_i < \beta_i$ for all indices i. The values $c_\alpha^{2\nu,\beta}$ do not depend on the data and have to be computed only once. From Eq. (13) we can construct the vector of coefficients $\mathbf{D}^{2\nu}$, Eq. (12), as follows:

$$\mathbf{D}^{2\nu} = C^{2\nu}\mathbf{D}, \quad \nu = 0, \ldots, \frac{n}{2}. \tag{15}$$

The $\frac{1}{2}(n+1)(n+2) \times \frac{1}{2}(n+1)(n+2)$ matrices $C^{2\nu}$ sum up to the identity:

$$\sum_{\nu=0}^{n/2} C^{2\nu} = I. \tag{16}$$

This decomposition gives the coefficient vector $\mathbf{D}^{2\nu}$ corresponding to a polynomial from the span of the spherical harmonics of order 2ν, $\{Y_{2\nu,m}(y), \ m = -2\nu, \ldots, 2\nu\}$. Since most approaches use properties of spherical harmonics, this decomposition allows one to use the same techniques in the tensor representation. We illustrate this point in the next section with several examples.

4 Applications

Example 1: Regularization. Laplace-Beltrami regularization is widely used in HARDI since it is a natural smoothing via diffusion on the sphere [11,12]. Let $S_n^{\text{SH}}(y)$ be a spherical harmonic decomposition of the signal S

$$S_n^{\text{SH}}(y) = \sum_{l=0}^{n} \sum_{m=-l}^{l} a_{lm} Y_{lm}(y), \tag{17}$$

and $\triangle_{\text{LB}}$ the Laplace-Beltrami operator on the unit sphere, then the regularized signal can be readily obtained [12]

$$S_n^{\text{SH}}(y,t) \equiv e^{t\triangle_{\text{LB}}} S_n^{\text{SH}}(y) = \sum_{l=0}^{n} \sum_{m=-l}^{l} a_{lm}(t) Y_{lm}(y), \tag{18}$$

where $a_{lm}(t) = e^{-l(l+1)t}a_{lm}$. Note that the coefficient transformation depends only on l and not on m. This allows us to apply this technique to the tensor representation. The polynomial with the coefficients $\mathbf{D}^{2\nu} = C^{2\nu}\mathbf{D}$ belongs to span of spherical harmonics of order 2ν. Therefore, the regularized polynomial will have the following coefficients

$$\mathbf{D}^{2\nu}(t) = e^{-2\nu(2\nu+1)t}C^{2\nu}\mathbf{D}. \tag{19}$$

The resulting regularization matrix for the whole polynomial is thus

$$C_{\mathrm{LB}}(t) = \sum_{\nu=0}^{n/2} e^{-2\nu(2\nu+1)t}C^{2\nu} \tag{20}$$

and the regularized polynomial can be written as

$$D(y_1, y_2, y_3, t) = \mathbf{D}^T C_{\mathrm{LB}}(t)\mathbf{v}, \tag{21}$$

The parameter t can be interpreted as inverse angular resolution. Figures 1 and 2 illustrate the importance of the scale parameter. In the case of noisy data, low t-values prevent correct detection of fiber orientations. In the interval $t \in [0.05, 0.15]$ the two most pronounced modes agree with the crossing fiber orientations with an angular error of less than $9°$, and a minimal error of $6°$.
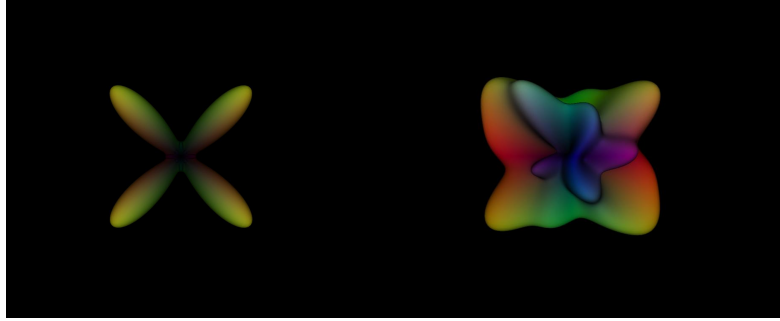
Fig. 1. Left: Synthetic noise-free profile induced by two crossing fibers at an angle of 90 degrees. Right: Same profile with added Rician noise.

Example 2: Q-Ball Imaging. A model-free diffusion ODF reconstruction scheme has been introduced by Tuch [10]. The diffusion probability function $P(\mathbf{r})$ is related to the measured MR diffusion signal $E(\mathbf{q})$, where $E(\mathbf{q}) = S(\mathbf{q})/S_0$ (S_0 is the non-diffusion-weighted image), by a Fourier integral

$$P = \mathcal{F}[E] \tag{22}$$
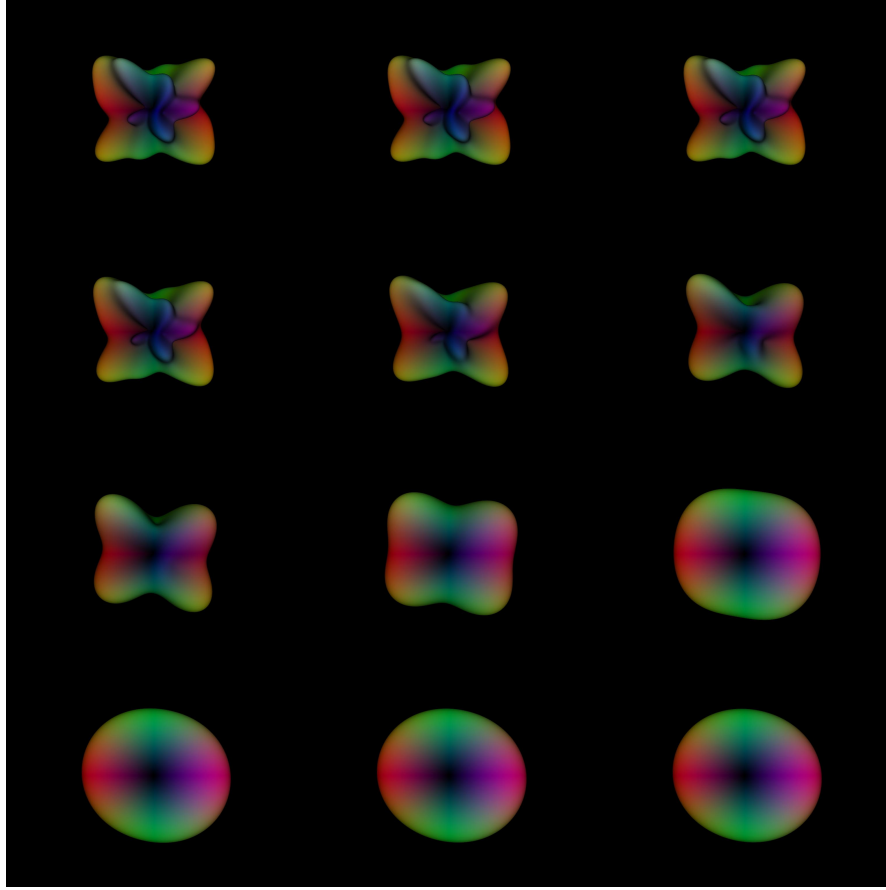
Fig. 2. Regularized profiles produced from the right image in Fig. 1 up to $n = 8$, with scale $t \in [0.007, 1.0]$ exponentially sampled.

where $\mathbf{r}$ is the displacement vector and $\mathbf{q}$ is the diffusion wave-vector, which is proportional to the applied magnetic field gradient in the MRI scanner. The three-dimensional probability density function $P(\mathbf{r})$ contains information about the tissue microstructure. A problem with using Eq. (22) directly via DFT is that acquisition data $E(\mathbf{q})$ for all $\mathbf{q}$ is needed. This is not feasible since it leads to long acquisition times and the need for high values of $|\mathbf{q}|$, causing serious noise problems. By considering the diffusion orientation function (ODF) for a direction $\mathbf{u}$ defined by the radial projection of the diffusion function

$$\Psi(u) = \int_0^\infty P(ru)\mathrm{d}r, \tag{23}$$

where u is a unit vector, the orientation structure of $P(\mathbf{r})$ can be described.

There are several similar analytical Q-ball algorithms [11,13,29]. In this example we use the approach of Descoteaux et al., based on the 3D Funk-Hecke theorem, since it

can be adopted for higher-order tensor representations. The Funk-Radon transform $\mathcal{G}$ of a spherical harmonic decomposition, Eq. (17), can now be written as

$$\Psi(u) = \mathcal{G}[S_n](u) = 2\pi \sum_{l=0}^{n} P_l(0) a_{lm} Y_{lm}(u). \tag{24}$$

where $P_{2\nu}(0) = (-1)^\nu \frac{(2\nu-1)!!}{(2\nu)!!}$ and the Funk-Radon transform is defined as

$$\mathcal{G}[f](u) \stackrel{\text{def}}{=} \int\int_{|w|=1} f(w)\delta(u^T w)\mathrm{d}w. \tag{25}$$

Here again the coefficient transformation depends only on the spherical harmonic order, and as in the regularization example, we can apply the result to our inhomogeneous tensor representation:

$$\mathbf{D}_{\text{ODF}}^{2\nu} = 2\pi P_{2\nu}(0) C^{2\nu} \mathbf{D}. \tag{26}$$

Therefore, we can construct the transformation matrix for the whole polynomial as

$$C_{\text{ODF}} = 2\pi \sum_{\nu=0}^{n/2} P_{2\nu}(0) C^{2\nu} \tag{27}$$

and finally we have

$$\Psi(u) = \mathbf{D}^T C_{\text{ODF}} \mathbf{v}, \tag{28}$$

The regularization and ODF reconstruction steps, given by Eqs. (18) and (28), can be combined in one for implementation purposes. Therefore, the whole algorithm for obtaining the diffusion ODF in tensor representation has two steps involving linear operations only:

1. Fit an nth order homogeneous polynomial to the signal by solving a linear system of equations.
2. Compute the regularized ODF coefficients $\mathbf{D}_{\text{ODF}}(t) = C_{\text{ODF}} C_{\text{LB}}(t) \mathbf{D}$.

Example 3: Constant Solid Angle Orientation Distribution Function. Several flaws of the Q-ball approach were pointed out in [30]. One of them is that the ODF definition does not deal with volume elements in a proper way, the adequate definition being

$$\Psi(u) = \int_0^\infty P(ru) r^2 \mathrm{d}r. \tag{29}$$

This definition has been used to compute the ODF in [8]. However, this approach is not model-free as it requires the Stejskal-Tanner assumption about monoexponential decay of the signal [31]. The modified formula for the ODF, say instead of Eq. (24), is

$$\Psi(u) = \frac{1}{4\pi} + \frac{1}{16\pi^2} \mathcal{G}[\triangle_{\text{LB}} \ln(-\ln(E(y)))](u), \tag{30}$$

In this case the same approach as in the original Q-ball gives

$$C_{\mathrm{ODF}} = -\frac{1}{8\pi} \sum_{\nu=0}^{n/2} P_{2\nu}(0) 2\nu(2\nu+1) C^{2\nu} \qquad (31)$$

and the final expression becomes

$$\Psi(u_1, u_2, u_3) = \frac{1}{4\pi} + \mathbf{D}^T C_{\mathrm{ODF}} \mathbf{v} \qquad (32)$$

where $\mathbf{D}$ is a vector of tensor coefficients of $\ln(-\ln(E(y)))$.

5   Conclusions

We have shown that a particular inhomogeneous polynomial representation of HARDI data on the unit sphere has certain theoretical and practical merits. We have derived the formulas for decomposition of a homogeneous polynomial of arbitrary order on the sphere in terms of such an inhomogeneous polynomial. The resulting decomposition requires a simple matrix multiplication of the vector of the coefficients obtained from the measurement data. We also show how this decomposition may be used for regularization and closed-form Q-ball representation. The resulting diffusion ODF is equivalent to the one obtained from the well-established analytical Q-ball algorithm. The advantage is that this approach does not require a detour via spherical harmonic decomposition, but instead can be obtained directly using a suitable higher order tensor formalism. This is of interest in many applications where the tensor formalism is the preferred choice.

The diffusion ODF can be used for fiber tracking techniques. In the most straightforward approach the tracking is performed by following the principle directions. For this reason maxima detection of the ODF is one of the major focuses, and a tensor representation has proven to be helpful [14,15]. We also would like to point out that in maxima detection techniques, regularization plays a crucial role. For this reason we have combined the Q-ball technique with regularization. In the case where the regularization parameter is sufficiently high, the blurred function has only one maximum. Decreasing regularization parameter leads to a splitting into two and subsequently more local maxima. Therefore, the hierarchical structure can be exploited in a coarse-to-fine maxima detection framework. Finally, the proposed method might also have applications in the context of Diffusional Kurtosis Imaging and in statistical models of second-order diffusion tensors, for decomposition of fourth-order kurtosis and covariance tensors.

References

1. Basser, P.J., Mattiello, J., Le Bihan, D.: Estimation of the effective self-diffusion tensor from the NMR spin echo. Journal of Magnetic Resonance **103** (1994) 247–254

2. Basser, P.J., Mattiello, J., Le Bihan, D.: MR diffusion tensor spectroscopy and imaging. Biophysics Journal **66**(1) (1994) 259–267

3. Tuch, D., Reese, T., Wiegell, M., Makris, N., Belliveau, J., van Wedeen, J.: High angular resolution diffusion imaging reveals intravoxel white matter fiber heterogeneity. Magnetic Resonance in Medicine **48**(6) (2004) 1358–1372

4. Alexander, D.C., Barker, G.J., Arridge, S.R.: Detection and modeling of non-Gaussian apparent diffusion coefficient profiles in human brain data. Magnetic Resonance in Medicine **48**(2) (2002) 331–340

5. Frank, L.R.: Characterization of anisotropy in high angular resolution diffusion-weighted MRI. Magnetic Resonance in Medicine **47**(6) (2002) 1083–1099

6. Özarslan, E., Mareci, T.H.: Generalized diffusion tensor imaging and analytical relationships between diffusion tensor imaging and high angular resolution imaging. Magnetic Resonance in Medicine **50** (2003) 955–965

7. Özarslan, E., Shepherd, T.M., Vemuri, B.C., Blackband, S.J., Mareci, T.H.: Resolution of complex tissue microarchitecture using the diffusion orientation transform (DOT). NeuroImage **31** (2006) 1086–1103

8. Aganj, I., Lenglet, C., Sapiro, G.: Odf reconstruction in q-ball imaging with solid angle consideration. In: ISBI'09: Proceedings of the Sixth IEEE international conference on Symposium on Biomedical Imaging, Piscataway, NJ, USA, IEEE Press (2009) 1398–1401

9. Tristan-Vega, A., Westin, C.F., Aja-Fernandez, S.: A new methodology for the estimation of fiber populations in the white matter of the brain with the funk-radon transform. NeuroImage **49** (2010) 1301–1315

10. Tuch, D.S.: Q-ball imaging. Magnetic Resonance in Medicine **52** (2004) 1358–1372

11. Descoteaux, M., Angelino, E., Fitzgibbons, S., Deriche, R.: Regularized, fast, and robust analytical Q-ball imaging. Magnetic Resonance in Medicine **58**(3) (2007) 497–510

12. Florack, L., Balmashnova, E.: Decomposition of high angular resolution diffusion images into a sum of self-similar polynomials on the sphere. In Bayakovsky, Y., Moiseev, E., eds.: Proceedings of the Eighteenth International Conference on Computer Graphics and Vision, GraphiCon'2008, Moscow, Russia, June 23–27, 2008, Moscow State University (2008) 26–31

13. Hess, C., Mukherjee, P., Han, E., Xu, D., Vigneron, D.: Q-ball reconstruction of multimodal fiber orientations using the spherical harmonic basis. Magnetic Resonance in Medicine **56**(1) (2006) 104–117

14. Bloy, L., Verma, R.: On computing the underlying fiber directions from the diffusion orientation distribution function. In Metaxas, D.N., Axel, L., Fichtinger, G., Székely, G., eds.: MICCAI (1). Volume 5241 of Lecture Notes in Computer Science., Springer (2008) 1–8

15. Ghosh, A., E.Tsigaridas, Descoteaux, M., Comon, P., B.Mourrain, Deriche, R.: A polynomial based approach to extract the maxima of an antipodally symmetric spherical function and its application to extract fiber directions from the orientation distribution function in diffusion mri. In: MICCAI:08 Workshop on Computational Diffusion MRI, New York, USA (10/09/2008 2008)

16. Özarslan, E., Vemuri, B., Mareci, T.: Generalized scalar measures for diffusion mri using trace, variance and entropy. In: Magn. Reson. Med. 53:866876. Biophysical Journal **94**(7) 28092818 O"zarslan et al. (2005)

17. Ghosh, A., Deriche, R.: Extracting geometrical features & peak fractional anisotropy from the ODF for white matter characterization. In: ISBI. (2011) 266–271

18. Fuster, A., van de Sande, J., Astola, L., Poupon, C., Velterop, J., ter Haar Romeny, B.M.: Fourth-order tensor invariants in high angular resolution diffusion imaging. In Zhang, G.H., Adluru, N., eds.: Proc. MICCAI Workshop on Computational Diffusion MRI. (2011) 54–63

19. A. Barmpoutis, M. S. Hwang, D.H.J.R.F., Vemuri, B.C.: Regularized positive-definite fourth-order tensor field estimation from dw-mri. NeuroImage **45**(1 sup.1) (March 2009) 153–162

20. Qi, L., Yu, Wu, E.X.: Higher order positive semidefinite diffusion tensor imaging. SIAM Journal on Imaging Sciences **3**(3) (2010) 416–433

21. Astola, L., Florack, L.: Finsler geometry on higher order tensor fields and applications to high angular resolution diffusion imaging. In Tai, X.C., Mørken, K., Lysaker, M., Lie, K.A., eds.: SSVM. Volume 5567 of Lecture Notes in Computer Science., Springer (2009) 224–234

22. Florack, L., Balmashnova, E., Astola, L., Brunenberg, E.: A new tensorial framework for single-shell high angular resolution diffusion imaging. Journal of Mathematical Imaging and Vision **3**(38) (August 13 2010) 171–181 Published online: DOI 10.1007/s10851-010-0217-3.

23. Melonakos, J., Pichon, E., Angenent, S., Tannenbaum, A.: Finsler active contours. IEEE Transactions on Pattern Analysis and Machine Intelligence **30**(3) (2008) 412–423

24. Descoteaux, M., Angelino, E., Fitzgibbons, S., Deriche, R.: Apparent diffusion coefficients from high angular resolution diffusion imaging: Estimation and applications. Magnetic Resonance in Medicine **56**(2) (2006) 395–410

25. Astola, L., Jalba, A., Balmashnova, E., Florack, L.: Finsler streamline tracking with single tensor orientation distribution function for high angular resolution diffusion imaging. Journal of Mathematical Imaging and Vision **41** (2011) 170–181

26. Florack, L., Balmashnova, E.: Two canonical representations for regularized high angular resolution diffusion imaging. In Alexander, D., Gee, J., Whitaker, R., eds.: MICCAI Workshop on Computational Diffusion MRI, New York, USA, September 10, 2008. (2008)

27. Descoteaux, M.: High angular resolution diffusion MRI: From local estimation to segmentation and tractography. In: PhD thesis. (2008)

28. Avery, J., Antonsen, F.: Evaluation of angular integrals by harmonic projection. Theoretical Chemistry Accounts: Theory, Computation, and Modeling **85**(1-3) (March 1993) 33–42

29. Anderson, A.W.: Measurement of fiber orienation distribution using angular resolution diffusion imaging. Magnetic Resonance in Medicine **54** (2005) 1194–1206

30. Barnett, A.: Theory of q-ball imaging redux: Implications for fiber tracking. Magnetic Resonance in Medicine **62**(4) (October 2009) 910–923

31. Stejskal, E.O., Tanner, J.E.: Spin diffusion measurements: Spin echoes in the presence of a time-dependent field gradient. Journal of Computational Physics **42** (1965) 288–292